JOURNAL OF SOLID STATE CHEMISTRY 35, 77–82 (1980)

Mössbauer Studies of Thiospinels. I. The System $FeCr_2S_4$–$FeRh_2S_4$

E. RIEDEL AND R. KARL

Institut für Anorganische und Analytische Chemie, Technische Universität Berlin, D-1000 Berlin 12, Germany

Received March 30, 1979; in revised form November 24, 1979

Spinel compounds $FeCr_{2-x}Rh_xS_4$ have been obtained as single-phase products for $0 \leq x \leq 1.2$. The ionic distribution is $Fe^{2+}[Cr^{3+}_{2-x}Rh^{3+}_x]S^{2-}_4$. Room-temperature Mössbauer spectra of ^{57}Fe consist of several overlapping doublets of almost identical isomer shifts but different quadrupole splittings which are attributed to tetrahedral Fe^{2+} with different numbers of Rh atoms as nearest octahedral site neighbors. The spectra have been compared with the unresolved doublet of Fe^{3+} in $Cu^{1+}_{0.5}Fe^{3+}_{0.5}[Cr^{3+}Rh^{3+}]S^{2-}_4$.

Introduction

The ferrimagnetic thiospinel $FeCr_2S_4$ has been subject of numerous studies (e.g., (*1*–*3*) and references therein), but only a few attempts have been made to investigate solid solutions with other thiospinels: $FeCr_2S_4$–$FeIn_2S_4$ (*4*), $FeCr_2S_4$–Fe_3S_4 (*2, 5*) and $FeCr_2S_4$–$CuCr_2S_4$ (*6, 7*). Together with the above systems we studied (*8*) the solid solution between $FeCr_2S_4$ and $FeRh_2S_4$. $FeRh_2S_4$ was claimed to be a spinel (*9, 10*), but its existence is doubtful (*11*). Here we present the results of our Mössbauer measurements on the mixed crystals $FeCr_{2-x}Rh_xS_4$.

Experimental

Preparation. Compounds of the series $FeCr_{2-x}Rh_xS_4$ were prepared by heating mixtures of the elements (99.9% or better) in evacuated silica ampoules. The mixtures were fired three or four times at 900–950°C for periods of 5 days. These conditions, leading to a minimum of impurities, were found during previous experiments at various temperatures. For a small sulfur deposit on the silica wall the sample was fired once more with a sulfur excess equivalent to the deposit. After each heating period the materials were cooled in the furnace and ground in an agate mortar.

Powder diffraction patterns were obtained with a Guinier–deWolff camera (CuK_α radiation) and with a Philips diffractometer (CrK_α radiation; external standard: gold). Cell dimensions were calculated with a precision of 0.2 pm using the Nelson–Riley extrapolation method. The cation distribution parameter and the anion shift parameter were determined from the intensities of the reflections with indices up to 642 as those with the lowest discrepancy factor $R = (\Sigma||F_o| - |F_c||)/\Sigma|F_c|$.

Seebeck measurements were performed between room temperature and 80°C with a Keithley voltmeter.

Mössbauer transmission spectra of ^{57}Fe were taken at room temperature with a conventional constant-acceleration spec-

0022-4596/80/130077-06$02.00/0

trometer (Elscint AME-30 comp.).[1] The absorber powder, about 5 mg Fe_{nat}/cm^2, was mounted in a Plexiglas holder (25-mm inner diameter). The source, ^{57}Co in Pd or Rh, was moved by a double-ended transducer. The velocity (symmetric triangular mode) was controlled by simultaneous accumulation of absolute velocity data produced by a laser interferometer. The cosine smearing effect was negligible. The Mössbauer and the velocity calibration spectra were accumulated in 500 channels each. The detector was a NaI(Tl) scintillation counter (Harshaw); the iron content of the entrance window was taken into account during the fitting procedure.

As routine analysis the spectra were fitted with a least-squares routine assuming Lorentzian lineshapes and equal intensities and half-widths of the doublet components. In some cases a routine compensating for the influence of the finite absorber thickness by numerical integration of the transmission integral was used ((*12*), "TI fits"). In general, no constraints were applied in the final fit; sometimes the linewidths of different singlets/doublets had to be held equal. The statistical reliability of the fit was measured by

$$\chi^2 = \sum_{1}^{500} (Y_0 - Y_c)^2/Y_0;$$

which was within the region 440–560 in all cases. Isomer shift values of fairly resolved lines could be reproduced with a precision of 0.001 mm/s; the absolute error is estimated to be less than 0.002 mm/s. All isomer shifts are reported relative to the gravity center of the metallic iron spectrum. In the figures, experimental count rates are shown as strokes according to their standard deviations, while straight or dashed lines correspond to calculated curves.

Results

Spinels of the series $FeCr_{2-x}Rh_xS_4$ with $0 \leq x \leq 1.2$ were obtained without appreciable impurities: the X-ray reflection intensity of foreign phases relative to the strongest spinel reflection is typically about 0.5%. Samples with $x > 1.2$ contain greater amounts of Rh_2S_3 and $Fe_{1-y}S$ phases; X-ray diagrams of $x = 2$ ($FeRh_2S_4$) show only weak spinel reflections. This result is consistent with (*11*) but contrasts with (*9, 10*). The cell edges *a* follow Vegard's law approximately (Table I). All spinels are found to be normal with only Fe^{2+} on tetrahedral sites. The anion shift parameter *u* has a constant value of 0.383 ± 0.001.

All materials are *p*-type semiconductors. The Seebeck coefficient decreases continuously as *x* increases (Table I).

The room-temperature Mössbauer spectrum (Fig. 1) of $FeCr_2S_4$ ($x = 0$) can be considered (*8*) mainly as a singlet or a weakly split doublet (isomer shift $\delta = 0.591$ mm/s; quadrupole splitting $\Delta \leq$

TABLE I

LATTICE PARAMETERS *a* AND SEEBECK COEFFICIENTS Θ OF $FeCr_{2-x}Rh_xS_4$ AT ROOM TEMPERATURE

x	*a* (pm)	Θ (μV/K)
0.0	999.8	483
0.03	999.7	—
0.06	999.5	—
0.1	999.2	477
0.2	998.5	—
0.3	997.8	349
0.4	997.4	—
0.5	996.8	300
0.6	996.1	212
0.8	995.2	175
1.0	994.4	153
1.2	993.5	140
1.5	991.9	—
2.0	989.1	—

---

[1] For a more detailed description see (*8*).

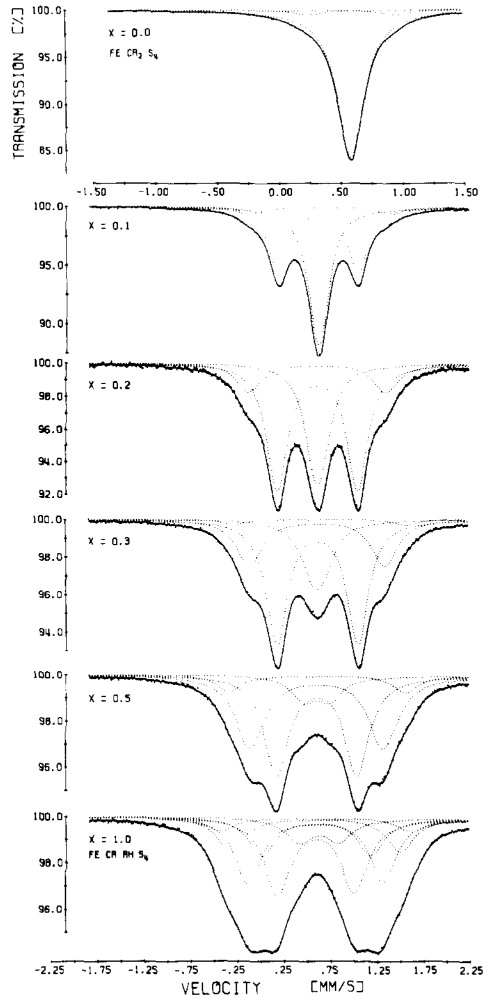

FIG. 1. Fitted Mössbauer spectra of $FeCr_{2-x}Rh_xS_4$ at room temperature.

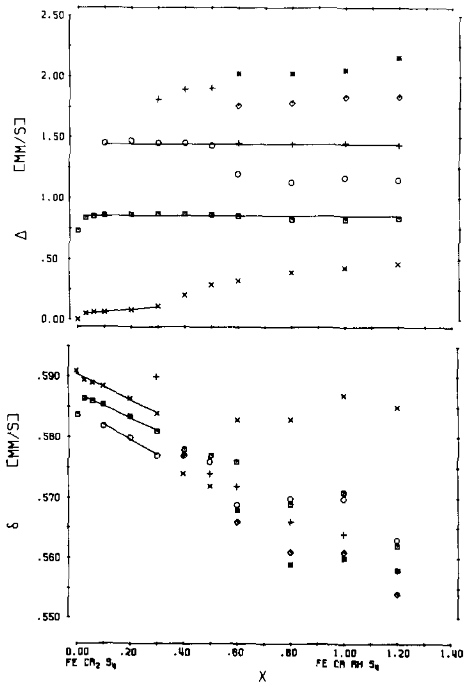

FIG. 2. Isomer shifts and quadrupole splittings of the component doublets $D1$-$D6$ (×, $D1$; □, $D2$; ○, $D3$; –, $D4$; ◇; *, $D6$).

mean isomer shift (shift of the gravity center) $\bar{\delta}$ is almost linear (Table II). The mean quadrupole splitting $\bar{\Delta}$ has its maximum value at $x = 1$. Values from TI fits are smaller than those from routine fits. Kondo (*10*), who prepared the compound $FeCrRhS_4$, found the following parameters: $\delta = 0.60$ mm/s, $\Delta = 1.1$ mm/s.

Data of all component doublets are shown in Fig. 2. The doublets are numbered $D1$, $D2$, . . . in the order of increasing Δ. For $x \leq 0.3$ the isomer shifts decrease in the direction $D1$-$D2$-$D3$. The differences are constant within experimental error: $\delta_{D1} - \delta_{D2} = \delta_{D2} - \delta_{D3} = 0.0033 \pm 0.0004$ mm/s. The value δ_{D2} for $x = 0$ is an exception to this rule, thus indicating that $D2$ of $x = 0$ does not correspond to $D2$ of $0 < x \leq 0.3$ (cf. footnote 2). The splittings of $D2$ and $D3$ for $0 < x \leq 0.5$ are constant (0.85 ± 0.01 mm/s and 1.44 ± 0.02 mm/s) and a very weak doublet ($\delta = 0.584$ mm/s, $\Delta = 0.702$ mm/s) in addition.[2] The spectra of the mixed crystals consist of several overlapping doublets of almost equal isomer shifts but different quadrupole splittings. The decrease of the

---

[2] $FeCr_2S_4$, whether polycrystalline or in single-crystal form, shows a weak nonstoichiometry. Small amounts of Fe^{3+} on octahedral sites result in a locally noncubic environment of some Fe^{2+}_T, thus leading to an additional doublet. A precise analysis will be given in another paper.

TABLE II

EXPERIMENTAL MÖSSBAUER DATA[a]

x	No. of doublets fitted	$\bar{\delta}$/Fe (mm/s)	$\bar{\Delta}$ (mm/s)	TI-$\bar{\Delta}$ (mm/s)	Γ (mm/s)
0.0	2	0.590	—	—	0.26
0.03	2	0.589	0.24	0.17	0.26
0.06	2	0.588	0.38	0.32	0.25–0.28
0.1	3	0.587	0.49	0.45	0.24–0.32
0.2	3	0.584	0.73	0.71	0.26–0.34
0.3	4	0.581	0.89	—	0.28–0.32
0.4	4	0.578	1.01	—	0.24–0.35
0.5	4	0.576	1.10	1.10	0.31–0.38
0.6	6	0.573	1.12	—	0.24–0.31
0.8	6	0.568	1.18	—	0.30
1.0	6	0.567	1.21	1.21	0.34
1.2	6	0.562	1.19	—	0.22–0.36

[a] Number of doublets fitted; mean isomer shift $\bar{\delta}$ (relative to iron metal); mean quadrupole splitting from routine fits and from TI fits, $\bar{\Delta}$ and TI-$\bar{\Delta}$; linewidth Γ.

0.02 mm/s, respectively) while the splitting of *D*1 increases—in the region $0.03 \leq x \leq 0.3$ linearly—with x.

Discussion

The shape of the Mössbauer spectra must be discussed on the basis of the normal cation distribution $Fe^{2+}[Cr^{3+}_{2-x}Rh^{3+}_{x}]S_4$ (the symbolism for valence distributions used in this publication does not imply the existence of isolated ions; the numbers describe the formal oxidation state only), which

—is expected because of the octahedral site preference of Cr^{3+} and Rh^{3+};

—has been established by the X-ray investigation.

In the course of the discussion, the weak additional doublet *D*2 in the spectrum of $FeCr_2S_4$ can be neglected; thereby the spectrum is reduced to a singlet of tetrahedral iron, Fe^{2+}_{T}, the usual interpretation. The similarity of the isomer shifts of all component doublets is further evidence that iron occupies tetrahedral sites only: octahedral iron, Fe^{2+}_{O}, is characterized by approximately 0.15 mm/s higher isomer shifts (e.g., (*4*)).

Due to the substitution of Rh_O for Cr_O the local environment of Fe_T is no longer cubic, so that appreciable quadrupole splittings arise (cf. (*2*)). The surprisingly strong quadrupole splittings of up to 2.15 mm/s can be interpreted in terms of different bonding characteristics of Cr_O and Rh_O. The bonds between Cr_O respectively Rh_O with sulfur exhibit a different degree of covalency and polarity. According to this model, charge differences between (a) Cr_O and Rh_O and (b) their respective sulfur neighbors will exist. As those sulfur atoms are also the direct neighbors of Fe_T, their influence on the resulting quadrupole splittings is believed to be more important. Nevertheless, this does not affect the following remarks, where for reasons of simplicity only the triggering octahedral cations are mentioned.

In the spinel lattice a tetrahedral site cation has

—12 nearest octahedral site neighbors at a distance $a(11/64)^{1/2}$,

—16 next-nearest octahedral site neighbors at a distance $a(27/64)^{1/2}$

apart from anions and tetrahedral site cations. The Mössbauer absorption of Fe_T in $FeCr_{2-x}Rh_xS_4$ is governed by the 12 nearest (Cr/Rh) neighbors. For $0 < x \leq 0.3$ the relation

$$D1 \mathrel{\hat{=}} \mathrm{Fe}(12\ \mathrm{Cr}/0\ \mathrm{Rh}),$$

$$D2 \mathrel{\hat{=}} \mathrm{Fe}(11\ \mathrm{Cr}/1\ \mathrm{Rh}),$$

$$D3 \mathrel{\hat{=}} \mathrm{Fe}(10\ \mathrm{Cr}/2\ \mathrm{Rh})$$

can be deduced from the isomer shifts: δ decreases linearly for each doublet according to the total Rh content. Moreover, each Rh nearest neighbor decreases δ by 0.0033 ± 0.0004 mm/s. This value is in agreement with the diminution of $\bar{\delta}$ from $x = 0$ to $x = 1$, where Fe_T is surrounded by 6 Cr and 6 Rh on the average. The diminution is 0.023 ± 0.003 mm/s, which is almost the same as $6 \cdot (0.0033 \pm 0.0004) = 0.020 \pm 0.002$ mm/s. The relationship between isomer shift and neighboring atoms has also been found in alloys (*13*).

The next-nearest neighbors exert minor influence, but cannot be neglected as can be seen from $\Delta_{D1} = 0.05 - 0.11$ mm/s. The increase with x is dependent on the number of next-nearest Rh neighbors. In contrast, Δ_{D2} and Δ_{D3} are constant (second neighbors cannot essentially change the average value of a large field gradient caused by the first neighbors).

Assuming random distribution of Cr and Rh on the octahedral sites, the frequencies of the configurations (12/0), (11/1), etc., can be calculated using the equation for binomial distributions. Table III compares such calculated values with the experimental data for the partial absorption areas of $D1$, $D2$, etc., in the range $0 < x \leq 0.3$. The values for $D1$ are in excellent agreement with those for a (12/0) surrounding, thus strongly supporting the basic conception. The correspondence between the data for $D2$, $D3$ and surroundings (11/1) respectively (10/2) is incomplete for $x \geq 0.1$, experimental areas of $D2$ being somewhat high, areas of $D3$ being low. Nevertheless, this behavior can be understood easily. It is obvious that $D1$ corresponds to a (12/0) neighborhood, so that all other doublets together represent all other neighborhoods. Among these, only the (11/1) sphere is expected to give rise to just one well-defined doublet. Configurations with two or more Rh neighbors create different quadrupole splittings contingent on the geometrical order of the Rh atoms. It can be shown (*14*) that some (10/2) configurations lead to a quadrupole splitting almost identical to that of (11/1). This will explain the observed deviations of the absorption areas of

TABLE III

PARTIAL MÖSSBAUER ABSORPTION AREAS[a]

	Partial absorption area of				Calculated frequency of the surrounding				
x	$D1$	$D2$	$D3$	$D4$	(12/0)	(11/1)	(10/2)	(9/3)	Other
0.03	0.84	0.16	—	—	0.834	0.152	0.013	0.001	—
0.06	0.67	0.33	—	—	0.694	0.258	0.044	0.004	—
0.1	0.55	0.39	0.06	—	0.540	0.341	0.099	0.017	0.003
0.2	0.30	0.55	0.15	—	0.282	0.377	0.230	0.085	0.026
0.3	0.19	0.53	0.25	0.03	0.142	0.301	0.292	0.172	0.093

[a] From TI fits (except for $x = 0.3$), and calculated frequencies of (Cr/Rh) surroundings for $Fe[Cr_{2-x}Rh_x]S_4$ (see text).

*D*2 and *D*3. On this basis the doublet assignment used so far can be given more precisely ($0 < x \leq 0.3$):

$D1 \hat{=} \mathrm{Fe(12\ Cr/0\ Rh)}$,

$D2 \hat{=} \mathrm{Fe(11\ Cr/1\ Rh)}$
+ some Fe(10 Cr/2 Rh),

$D3 \hat{=}$ remaining Fe(10 Cr/2 Rh).

This refined assignment has no overall effect on the validity of the estimation of isomer shift changes due to neighboring atoms derived earlier. The surroundings with three or more Rh atoms, for small x less abundant, are likely to create a large variety of different quadrupole splittings which evidently cannot be found as separate doublets in the spectra; their contributions are partially represented by *D*4 and partially underlie the other doublets. For higher x and hence increasing diversity of possible configurations an assignment of specific surroundings to certain doublets becomes unreasonable.

Comparison with $\mathrm{Cu_{0.5}Fe_{0.5}CrRhS_4}$

According to a model by Lotgering *et al.* (*7*) the above compound can be described by $\mathrm{Cu^{1+}_{0.5}Fe^{3+}_{0.5}[Cr^{3+}Rh^{3+}]S^{2-}_4}$; hence it contains $\mathrm{Fe^{3+}}$ instead of $\mathrm{Fe^{2+}}$. In order to compare these two situations we prepared this compound using the described techniques. The material (a = 986.6 pm, u = 0.383; no extraneous or superstructure lines) exhibits a "single line" Mössbauer spectrum: $\delta = 0.313$ mm/s, Δ h 0.13 mm/s, $\Gamma = 0.27$ mm/s.

Usually the EFG is separated into a lattice contribution q_L (from surrounding charges) and a valence contribution q_V (from the electrons of the Mössbauer atom) (*15*). If the electrons in the valence shell of the Mössbauer atom have cubic symmetry—as in high-spin $\mathrm{Fe^{3+}_T}$ with $e^2t_2^3$ configuration—q_V is zero. Therefore the quadrupole splitting in $\mathrm{Cu_{0.5}Fe^{3+}_{0.5}[CrRh]S_4}$ arises from q_L; this means that the direct influence of the differently charged neighbors is measured. In the series $\mathrm{Fe^{2+}[Cr_{2-x}Rh_x]S_4}$, the $e^3t_2^3$ configuration splits up further, the spherical symmetry is removed, and the lattice contribution is strongly amplified by the valence shell of $\mathrm{Fe^{2+}_T}$.

Acknowledgment

The authors are indebted to Professor P. Gütlich, Joh. Gutenberg-University of Mainz, for parts of the fitting routine.

References

1. M. R. Spender and A. H. Morrish, *Solid State Commun.* **11**, 1417 (1972).
2. F. K. Lotgering, A. M. van Diepen and J. F. Olijhoek, *Solid State Commun.* **17**, 1149 (1975); *J. Magn. Magn. Mater.* **3**, 117 (1976).
3. P. Gibart, L. Goldstein, and L. Brossard, *J. Magn. Magn. Mater.* **3**, 109 (1976).
4. L. Brossard, L. Goldstein, and M. Guittard, *J. Phys.* (*Paris*) **37**, C6-493 (1976); L. Goldstein, L. Brossard, M. Guittard, and J.-L. Dormann, *Physica 86–88B*, 889 (1977).
5. M. Robbins, R. Wolff, A. J. Kurtzig, R. C. Sherwood, and M. A. Miksovsky, *J. Appl. Phys.* **41**, 1086 (1970).
6. G. Haacke and L. C. Beegle, *J. Appl. Phys.* **39**, 656 (1968); G. Haacke and A. J. Nozik, *Solid State Commun.* **6**, 363 (1968).
7. F. K. Lotgering, R. P. van Stapele, G. H. A. M. van der Steen and J. S. van Wieringen, *J. Phys. Chem. Solids* **30**, 799 (1969).
8. R. Karl, Thesis, TU Berlin, Berlin 1978, D 83.
9. G. Blasse and D. J. Schipper, *J. Inorg. Nucl. Chem.* **26**, 1467 (1964).
10. H. Kondo, *J. Phys. Soc. Japan* **41**, 1247 (1976).
11. R. E. Tressler and V. S. Stubican, *Nat. Bur. Stand.* (*U.S.*), *Spec. Publ.* **364**, 695 (1972); R. E. Tressler, F. A. Hummel, and V. S. Stubican, *J. Amer. Ceram. Soc.* **51**, 648 (1968).
12. T. E. Cranshaw, *J. Phys. E* **7**, 122 (1974).
13. F. E. Fujita, *in* "Mössbauer Spectroscopy" (U. Gonser, Ed.), Topics in Applied Physics, Vol. 5, Springer-Verlag, Berlin/Heidelberg/New York (1975).
14. E. Riedel and R. Karl, to be published.
15. G. M. Bancroft, "Mössbauer Spectroscopy," Chap. 2, McGraw–Hill, London (1973); G. M. Bancroft and R. H. Platt, *Advan. Inorg. Chem. Radiochem.* **15**, 59 (1972).